



HAL
open science

Effect of temperature anisotropy on the dynamics of geodesic acoustic modes

J.N. Sama, A. Biancalani, A. Bottino, I. Chavdarovski, D. Del Sarto, A. Ghizzo, T. Hayward-Schneider, Ph. Lauber, B. Rettino, F. Vannini

► **To cite this version:**

J.N. Sama, A. Biancalani, A. Bottino, I. Chavdarovski, D. Del Sarto, et al.. Effect of temperature anisotropy on the dynamics of geodesic acoustic modes. *Journal of Plasma Physics*, 2023, 89 (1), pp.905890109. 10.1017/S0022377823000016 . hal-04561941

HAL Id: hal-04561941

<https://hal.science/hal-04561941>

Submitted on 28 Apr 2024

HAL is a multi-disciplinary open access archive for the deposit and dissemination of scientific research documents, whether they are published or not. The documents may come from teaching and research institutions in France or abroad, or from public or private research centers.

L'archive ouverte pluridisciplinaire **HAL**, est destinée au dépôt et à la diffusion de documents scientifiques de niveau recherche, publiés ou non, émanant des établissements d'enseignement et de recherche français ou étrangers, des laboratoires publics ou privés.

Journal:	<i>Journal of Plasma Physics</i>
Manuscript ID	Draft
Manuscript Type:	
Date Submitted by the Author:	n/a
Complete List of Authors:	Sama, Juvert Njeck; University of Lorraine,
Keywords:	
Abstract:	

SCHOLARONE™
Manuscripts

Effect of temperature anisotropy on the dynamics of geodesic acoustic modes

J.N Sama¹†, A. Biancalani^{2,3}, A. Bottino³, I. Chavdarovski⁴, D. Del Sarto¹, A. Ghizzo¹, T. Hayward-Schneider³, P. Lauber³, B. Rettino³ and F. Vannini³

¹Institut Jean Lamour UMR 7198, Université de Lorraine-CNRS, Nancy, France

²Léonard de Vinci Pôle Universitaire, Research Center, Paris La Défense, France

³Max Planck Institute for Plasma Physics, Garching, Germany

⁴Korea Institute of Fusion Energy, Daejeon, South Korea

(Received xx; revised xx; accepted xx)

In this work, we revisit the linear gyro-kinetic theory of geodesic acoustic modes (GAMs) and derive a general dispersion relation for an arbitrary equilibrium distribution function of ions. A bi-Maxwellian distribution of ions is then used to study the effects of ion temperature anisotropy on GAM frequency and growth rate. We find that ion temperature anisotropy yields sensible modifications to both the GAM frequency and growth rate as both tend to increase with anisotropy and these results are strongly affected by the electron to ion temperature ratio.

1. Introduction

Geodesic acoustic modes (GAMs) (Winsor *et al.* 1968), are oscillating axisymmetric perturbations that are unique to configurations with closed magnetic field lines with a geodesic curvature, like tokamaks. They are the oscillating counterparts of the zero frequency zonal flow (ZFZF) (Hasegawa *et al.* 1979) and are examples of zonal structures. Zonal structures are of great interest to magnetic fusion reactors due to their potential capabilities of generating non-linear equilibrium (Chen & Zonca 2007) by regulating microscopic turbulence and its associated heat and particle transport.

GAMs have been largely studied in literature, both analytically (see Qiu *et al.* 2009; Hassam & Kleva 2011; Smolyakov *et al.* 2008; Zonca & Chen 2008; Girardo *et al.* 2014; Garbet *et al.* 2006; Chakrabarti *et al.* 2010; Zarzoso *et al.* 2012; Gao 2013; Ming *et al.* 2018; Zhang & Zhou 2010; Ren 2015; Conway *et al.* 2022) and numerically (see Biancalani *et al.* 2014; Grandgirard *et al.* 2019; Novikau *et al.* 2017). A key aspect in the linear gyro-kinetic theory of GAMs is the determination of mode frequency and damping rate. The GAM frequency is of the order of the ion sound frequency, and its major damping mechanism is collisionless damping. Analytical expressions of GAM frequency and growth rate, can be found, for example, in (Sugama & Watanabe 2006; Qiu *et al.* 2009). These expressions were obtained assuming Maxwellian distributions of ions and electrons with no temperature anisotropy.

Tokamak plasmas are generally modeled in analytical theory, assuming isotropic Maxwellian distributions of ions and electrons. However, in reality, there can be several sources of anisotropy in tokamak plasmas. Anisotropy in tokamaks can be introduced by auxiliary heating such as neutral beam injection (NBI), which can generate a strong parallel temperature anisotropy, whereas strong perpendicular temperature anisotropy

† Email address for correspondence: juvert-njeck.sama@univ-lorraine.

can be observed when using ion cyclotron resonance heating (ICRH). Parallel and perpendicular here are defined with respect to the equilibrium magnetic field. Generally, ion temperature anisotropy, both gyrotropic and non-gyrotropic can be generated due to the action of the traceless rate of shear, which anisotropically heats the in-plane components of the pressure tensor by tapping kinetic energy from shear flow, when the local gradient of the ion fluid velocity, say $\omega \sim \|\nabla \mathbf{u}_i\|$, is not negligible with respect to the local ion cyclotron frequency Ω_i and the collision rate (Del Sarto *et al.* 2016). This condition is likely to occur in developed turbulence, since it can be verified on the vorticity sheets delimiting vortex structures (Del Sarto & Pegoraro 2018*a*). In particular, as long as the ratio ω/Ω_i , remains small enough, the generated anisotropy is mostly gyrotropic and thus compatible with a gyrokinetic description (Del Sarto & Pegoraro 2018*b*) and it can be thus related to the first order finite-Larmor radius corrections to double-adiabatic closures (Kaufman 1960; Thompson 1961; Macmahon 1965; Cerri *et al.* 2013). Sasaki *et al.* (1997) measured reasonably high ion temperature anisotropy in EXTRAP-T2, and large pressure anisotropies have also been reported in (Hole *et al.* 2001, 2011). Ren & Cao (2014) studied the impact of ion temperature anisotropy on GAM frequency and growth rate in the limit of a vanishing electron to ion temperature ratio, with ions described by a bi-Maxwellian distribution. These authors found that ion temperature anisotropy modifies the linear dynamics of GAMs. However, the GAM dynamics is known to strongly depend on the electron to ion temperature ratio (see Qiu *et al.* 2009; Zonca & Chen 2008; Biancalani *et al.* 2014; Sugama & Watanabe 2006). Hence, a finite electron to ion temperature ratio must be retained in a complete linear theory of GAMs.

In this work, we investigate the linear dynamics of GAMs with a bi-Maxwellian distribution of ions and assuming adiabatic electrons, as in (Zonca & Chen 2008; Sugama & Watanabe 2006). We generalize the work of Ren & Cao (2014), to a general value of electron to ion temperature ratio and by keeping account of a gyro-tropic ion temperature anisotropy, using an approach based on the standard limit of small finite-orbit-radius and small finite-orbit-width, kept up to the leading order (consistently with Zonca *et al.* (1996); Zonca & Chen (2008)). We show that in the appropriate limits, we recover the GAM dispersion derived in (Ren & Cao 2014; Zonca & Chen 2008; Girardo *et al.* 2014) from the general GAM dispersion relation which we here obtain. From our study, we find that the ion temperature anisotropy yields a sensible modification to both the real and imaginary part of the frequency, as both tend to be increasing functions of $\chi = \frac{T_{\perp,i}}{T_{\parallel,i}}$, and this result is strongly affected by the electron to ion temperature ratio, $\tau = \frac{T_e}{T_i}$. The equivalent ion temperature T_i , is defined such that it corresponds to the same total pressure as that of the anisotropic distribution ($T_i = \frac{T_{\parallel,i}}{3} + \frac{2T_{\perp,i}}{3}$).

The first section of our work is an introduction, which describes the motivations for this work. In the second section, we derive a general linear GAM dispersion relation for an arbitrary distribution function. In section three, we solve the dispersion relation with a bi-Maxwellian distribution of ions and study the impact of ion temperature anisotropy and electron to ion temperature ratio on GAM frequency and growth rate. We apply our theory to an experimentally relevant case in section four and conclusions are reported in section five.

2. The model for a general distribution function

In this section, we use the gyro-kinetic formalism to study the physics of GAMs in the electrostatic limit. The fundamental equations of this model are the gyro-kinetic Vlasov

equation (2.1) and Poisson equations (2.2).

$$\frac{\partial f_s}{\partial t} + \dot{\mathbf{R}} \cdot \frac{\partial f_s}{\partial \mathbf{R}} + \dot{E} \frac{\partial f_s}{\partial E} = 0 \quad (2.1)$$

$$-\nabla \cdot \left(\frac{n_{0,i} m_i c^2}{B^2} \nabla_{\perp} \Phi \right) = \int dW_i Z_i e J_{0,i} f_i - \int dW_e e f_e \quad (2.2)$$

where f_s , is the distribution function of a given species, \vec{R} is the particle position vector, $E = \frac{m_s}{2} (v_{\parallel}^2 + v_{\perp}^2)$, is the particle energy, e , the electron charge, $n_{0,s}$, the equilibrium density of a species s , m , particle mass, c , speed of light, B , magnitude of magnetic field, Z_s , species charge number, $J_{0,i}$, ion gyro-average operator and dW_s , is the volume element in velocity space.

We make the following assumptions,

- (i) We consider adiabatic electrons.
- (ii) Neglect magnetic fluctuations.
- (iii) Use flat density and temperature profiles.

2.1. Linear analysis

We linearize the Vlasov and quasi-neutrality equation by splitting each quantity into an equilibrium and a perturbed component such that,

$$f_s = f_{0,s} + f_{1,s} \quad (2.3)$$

$$\dot{\mathbf{R}} = \dot{\mathbf{R}}_0 + \dot{\mathbf{R}}_1 \quad (2.4)$$

$$\dot{E} = \dot{E}_0 + \dot{E}_1 \quad (2.5)$$

$$\Phi = \Phi_1 \quad (2.6)$$

Where $\dot{\mathbf{R}}_0$ is the unperturbed particle velocity *i.e.* $\dot{\mathbf{R}}_0 = \mathbf{v}_{\parallel} + \mathbf{v}_{\nabla B} + \mathbf{v}_{curvB}$ and $E_0 = \frac{m(v_{\parallel}^2 + v_{\perp}^2)}{2}$.

Linear Vlasov equation

Substituting equation (2.3)-(2.6) in (2.1), and neglecting second and higher order terms, the linear Vlasov equation reads,

$$\frac{\partial f_{1,s}}{\partial t} + \dot{\mathbf{R}}_0 \cdot \frac{\partial f_{1,s}}{\partial \mathbf{R}} = -\dot{E}_1 \frac{\partial f_{0,s}}{\partial E} \quad (2.7)$$

This linear Vlasov equation can be further simplified by splitting the perturbed distribution function into an adiabatic and a non-adiabatic component,

$$f_{1,s} = E_1 \frac{\partial f_{0,s}}{\partial E} + h_s \quad (2.8)$$

Substituting equation (2.8) in (2.7), we obtain the equation for the non-adiabatic part of the perturbed distribution function,

$$\frac{\partial h_s}{\partial t} + \dot{\mathbf{R}}_0 \cdot \frac{\partial h_s}{\partial \mathbf{R}} = -\dot{E}_1 \frac{\partial f_{0,s}}{\partial E} \quad (2.9)$$

Using the expression of the equilibrium velocity and perturbations of the form $x \rightarrow \exp(ik_r - i\omega t) + c.c.$, in equation (2.9) we obtain the expression,

$$\left(\omega_{t,s} \frac{\partial}{\partial \theta} - i(\omega + \omega_{d,s}) \right) h_s = i\omega E_1 \frac{\partial f_{0,s}}{\partial E} \quad (2.10)$$

Where, $\omega_t = \frac{v_{||}}{qR_0}$, is the transit frequency, q is the safety factor, $\omega_{d,s} = \bar{\omega}_{d,s} \sin \theta$, is the drift frequency with, $\bar{\omega}_{d,s} = \frac{cm_s k_r}{Z_s e B_0 R_0} \left(v_{||}^2 + \frac{v_{\perp}^2}{2} \right)$, $E_1 = Z_s e J_{0,s} \bar{\Phi}_1$ and k_r is the radial wave number. Since GAMs are predominantly zonal, we can further divide the non-adiabatic part of the perturbed distribution function into a zonal and a non-zonal part,

$$h = \bar{h} + \delta h \quad (2.11)$$

similarly, we write the scalar potential as,

$$\Phi_1 = \bar{\Phi} + \tilde{\Phi} \quad (2.12)$$

where the overhead bar represents the zonal components. Using these definitions, and making a flux surface average of the gyro-kinetic equation to eliminate the zonal component of the non-adiabatic part of the perturbed distribution function, the linear Vlasov equation reduces to,

$$\left(\omega_{t,s} \frac{\partial}{\partial \theta} - i(\omega + \omega_{d,s}) \right) \delta h_s = i Z_s \frac{\partial f_{0,s}}{\partial E} \left(\omega J_{0,s} \tilde{\Phi} - \omega_{d,s} J_{0,s} \bar{\Phi} \right) \quad (2.13)$$

The corresponding vorticity equation is obtained by multiplying this relation by the gyro-average operator and integrating over the velocity space.

$$\left\langle J_{0,s} \left(\omega_{t,s} \frac{\partial}{\partial \theta} - i(\omega + \omega_{d,s}) \right) \delta h_s \right\rangle_W = \left\langle i Z_s \frac{\partial f_{0,s}}{\partial E} \left(\omega J_{0,s}^2 \tilde{\Phi} - \omega_{d,s} J_{0,s}^2 \bar{\Phi} \right) \right\rangle_W \quad (2.14)$$

Considering all the changes of variable we have made, the perturbed distribution function has the form,

$$f_{1,s} = Z_s e J_{0,s} \frac{\partial f_{0,s}}{\partial E} \tilde{\Phi} + \delta h_s \quad (2.15)$$

Linear quasi-neutrality equation

Using a similar approach, we substitute equations (2.3) and (2.6) into (2.2) and we thus obtain the equation below,

$$\frac{m_i c^2}{B^2} k_r^2 \bar{\Phi} = e^2 \left\langle J_{0,i}^2 \frac{\partial f_{0,i}}{\partial E} \right\rangle_W \left(1 + \frac{\left\langle J_{0,e}^2 \frac{\partial f_{0,e}}{\partial E} \right\rangle_W}{\left\langle J_{0,i}^2 \frac{\partial f_{0,i}}{\partial E} \right\rangle_W} \right) \tilde{\Phi} + e \langle J_{0,i} \delta h_i \rangle_W \quad (2.16)$$

where $\langle \dots \rangle_W$, represent the integral over velocity space. The non-adiabatic part of the perturbed electron distribution function has been neglected in accordance with our assumptions.

2.2. Ordering of the gyro-kinetic equation

The gyro-kinetic equation (2.13) describes a wide range of phenomena at different time scales. In order to study GAMs, we need to apply an appropriate ordering that will filter out time scales which are irrelevant to GAM dynamics. The GAM frequency is of the order of ion sound frequency. The ordering is done by comparing this frequency with the characteristic frequencies in our system *i.e.* $\omega_{t,s}$, $\omega_{d,s}$.

$$\frac{\omega_{t,i}}{\omega} \sim O(1), \quad \frac{\omega_{d,i}}{\omega} \sim O(\epsilon), \quad \frac{\delta h_i}{f_{0,i}} \sim O(\epsilon) \quad (2.17)$$

$$\frac{\omega_{t,e}}{\omega} \gg 1, \quad \frac{\omega_{d,e}}{\omega} \sim O(1), \quad \frac{\delta h_e}{f_{0,e}} \sim O(\epsilon) \quad (2.18)$$

In the leading order, the ion and electron gyro-kinetic equations are respectively,

$$\left(\frac{\omega_{t,i}}{\omega} \frac{\partial}{\partial \theta} - i \right) \delta h_i = i Z_i e \frac{\partial f_{0,i}}{\partial E} \left(J_{0,i} \tilde{\Phi} - J_{0,i} \frac{\omega_{d,i}}{\omega} \bar{\Phi} \right) \quad (2.19)$$

$$\delta h_e = 0 \quad (2.20)$$

2.3. General form of dispersion relation

We consider the following form for the non-zonal perturbed ion distribution function and scalar potential.

$$\tilde{\Phi} = \tilde{\Phi}_s \sin \theta + \tilde{\Phi}_c \cos \theta \quad (2.21)$$

$$\delta h_i = \delta h_{i,s} \sin \theta + \delta h_{i,c} \cos \theta \quad (2.22)$$

Substituting these relations into equation (2.19) and separating the sine and cosine components, we obtain,

$$\delta h_{i,s} = \frac{i Z_i J_{0,i} \frac{\partial f_{0,i}}{\partial E}}{\left(\frac{\omega_{t,i}}{\omega} \right)^2 - 1} \left[-i \left(\tilde{\Phi}_s - \left(\frac{\bar{\omega}_{d,i}}{\omega} \right) \bar{\Phi} \right) + \frac{\omega_{t,i}}{\omega} \tilde{\Phi}_c \right] \quad (2.23)$$

$$\delta h_{i,c} = -\frac{i Z_i J_{0,i} \frac{\partial f_{0,i}}{\partial E}}{\left(\frac{\omega_{t,i}}{\omega} \right)^2 - 1} \left[\frac{\omega_{t,i}}{\omega} \left(\tilde{\Phi}_s - \left(\frac{\bar{\omega}_{d,i}}{\omega} \right) \bar{\Phi} \right) + i \tilde{\Phi}_c \right] \quad (2.24)$$

Following the same procedure with the quasi-neutrality equation,

$$\tilde{\Phi}_c = -\frac{\langle J_{0,i} \delta h_{i,c} \rangle_W}{e \langle J_{0,i}^2 \frac{\partial f_{0,i}}{\partial E} \rangle_W \left(1 + \frac{\langle J_{0,e}^2 \frac{\partial f_{0,e}}{\partial E} \rangle_W}{\langle J_{0,i}^2 \frac{\partial f_{0,i}}{\partial E} \rangle_W} \right)} \quad (2.25)$$

$$\tilde{\Phi}_s = -\frac{\langle J_{0,i} \delta h_{i,s} \rangle_W}{e \langle J_{0,i}^2 \frac{\partial f_{0,i}}{\partial E} \rangle_W \left(1 + \frac{\langle J_{0,e}^2 \frac{\partial f_{0,e}}{\partial E} \rangle_W}{\langle J_{0,i}^2 \frac{\partial f_{0,i}}{\partial E} \rangle_W} \right)} \quad (2.26)$$

Taking the flux surface average of the quasi-neutrality equation (2.19) and the vorticity equation (2.14) we have respectively,

$$\frac{m_i c^2}{B^2} k_r^2 \bar{\Phi} = e \overline{\langle J_{0,i} \delta h_i \rangle}_W \quad (2.27)$$

$$\overline{\langle J_{0,i} \delta h_i \rangle}_W = -\frac{\overline{\langle J_{0,i} \omega_{d,i} \delta h_i \rangle}_W}{\omega} \quad (2.28)$$

Substituting equation (2.28) into (2.27) and evaluating the flux surface average, we obtain,

$$\frac{2m_i}{B^2} k_r^2 \bar{\Phi} = -\frac{e}{c^2 \omega} \langle J_{0,i} \bar{\omega}_{d,i} \delta h_{i,s} \rangle \quad (2.29)$$

Substituting equation (2.23), we obtain the general dispersion relation of GAMs in the leading order,

$$\frac{2m_i c^2 k_r^2}{B^2} \bar{\Phi} = -e^2 \omega \left\langle \frac{J_{0,i}^2 \bar{\omega}_{d,i} \frac{\partial f_{0,i}}{\partial E}}{\omega_{t,i}^2 - \omega^2} \right\rangle_W \tilde{\Phi}_s + e^2 \left\langle \frac{J_{0,i}^2 \bar{\omega}_{d,i}^2 \frac{\partial f_{0,i}}{\partial E}}{\omega_{t,i}^2 - \omega^2} \right\rangle_W \bar{\Phi} \quad (2.30)$$

3. Case of bi-Maxwellian

3.1. Derivation of dispersion relation

To evaluate the integrals over the velocity space given in the general linear GAM dispersion relation equation (2.30), we have to choose an equilibrium distribution function for ions. In this work, we consider it to be a bi-Maxwellian, while a regular Maxwellian is used for electrons. The ion distribution function is normalized such that its integral over velocity space equals one ($n_{0,i} = 1$). We take $J_{0,i} = 1$ (drift kinetic limit).

$$f_{0,i} = \left(\frac{m_i}{2\pi T_{\parallel}} \right)^{\frac{1}{2}} \left(\frac{m_i}{2\pi T_{\perp}} \right) \exp \left[-\frac{m_i}{2} \left(\frac{v_{\parallel}^2}{T_{\parallel}} + \frac{v_{\perp}^2}{T_{\perp}} \right) \right] \quad (3.1)$$

By defining an equivalent temperature, $T_i = \frac{T_{\parallel,i}}{3} + \frac{2T_{\perp,i}}{3}$, the bi-Maxwellian can be written in the form,

$$f_{0,i} = \frac{b^{\frac{3}{2}}}{\pi^{\frac{3}{2}} v_t^3 \chi} \exp \left[-b \left(\frac{v_{\parallel}^2 + v_{\perp}^2 \chi^{-1}}{v_t^2} \right) \right] \quad (3.2)$$

Where $b = \frac{2\chi+1}{T_i}$, with $\chi = \frac{T_{\perp,i}}{T_{\parallel,i}}$, $v_t = \sqrt{\frac{2T_i}{m}}$ and $E = \frac{m}{2} (v_{\parallel}^2 + v_{\perp}^2)$. we have,

$$\frac{\partial f_{0,i}}{\partial E} = -\frac{b}{T_i} f_{0,i} \quad (3.3)$$

Equation (2.26) then reduces to,

$$\tilde{\Phi}_s = \frac{\omega \left\langle \frac{\bar{\omega}_{d,i} f_{0,i}}{\omega_t^2 - \omega^2} \right\rangle_W}{1 + \frac{1}{\tau b} + \omega^2 \left\langle \frac{f_{0,i}}{\omega_t^2 - \omega^2} \right\rangle_W} \bar{\Phi} \quad (3.4)$$

Where $\tau = \frac{T_e}{T_i}$. Substituting this result in the general dispersion relation, we have,

$$\frac{2m_i c^2 k_r^2}{B^2} + \frac{e^2 b}{T_i} \left[\left\langle \frac{\bar{\omega}_{d,i}^2 f_{0,i}}{\omega_t^2 - \omega^2} \right\rangle_W - \frac{\omega^2 \left\langle \frac{\bar{\omega}_{d,i} f_{0,i}}{\omega_t^2 - \omega^2} \right\rangle_W^2}{1 + \frac{1}{\tau b} + \omega^2 \left\langle \frac{f_{0,i}}{\omega_t^2 - \omega^2} \right\rangle_W} \right] = 0 \quad (3.5)$$

These three velocity integrals once evaluated read,

$$\left\langle \frac{\bar{\omega}_{d,i} f_{0,i}}{\omega_t^2 - \omega^2} \right\rangle_W = \frac{cm_i k_r v_t^2}{eB_0 R_0 b \omega_0^2 y} \left[y + \left(\frac{\chi}{2} + y^2 \right) Z(y) \right] \quad (3.6)$$

$$\left\langle \frac{\bar{\omega}_{d,i}^2 f_{0,i}}{\omega_t^2 - \omega^2} \right\rangle_W = \left(\frac{cm_i k_r v_t^2}{eB_0 R_0 b} \right)^2 \frac{1}{\omega_0^2 y} \left[\frac{y}{2} + y^3 + y\chi + \left(\frac{\chi^2}{2} + \chi y^2 + y^4 \right) Z(y) \right] \quad (3.7)$$

$$\left\langle \frac{f_{0,i}}{\omega_t^2 - \omega^2} \right\rangle_W = \frac{1}{\omega_0^2} \frac{Z(y)}{y} \quad (3.8)$$

Where $Z(y)$ is the plasma dispersion function and,

$$y = \frac{\omega}{\omega_0}, \quad \omega_0 = \frac{v_t}{qR_0 \sqrt{b}}$$

Then equation (3.5) becomes,

$$y + q^2 \left[F(y) - \frac{N^2(y)}{D(y)} \right] = 0 \quad (3.9)$$

With,

$$F(y) = \frac{y}{2} + y^3 + y\chi + \left(\frac{\chi^2}{2} + y^2\chi + y^4 \right) Z(y) \quad (3.10)$$

$$N(y) = y + \left(\frac{\chi}{2} + y^2 \right) Z(y) \quad (3.11)$$

$$D(y) = \frac{1}{y} \left(1 + \frac{1}{\tau b} \right) + Z(y) \quad (3.12)$$

3.2. Comparison with fluid limit and with previous results

In the limit $\chi = 1$, we recover the GAM dispersion relations in (Zonca & Chen 2008; Zonca *et al.* 1996; Girardo *et al.* 2014). In the fluid limit, we can show that, the dispersion relation equation (3.9), reduces to,

$$\omega^2 = \left(\frac{3}{4} + \frac{\chi}{2} + \frac{\chi^2}{2} + b\tau \left(\frac{\chi^2}{4} + \frac{\chi}{2} + \frac{1}{4} \right) \right) \frac{v_t^2}{bR_0^2} \quad (3.13)$$

If we consider the isotropic limit of this fluid dispersion relation, we obtain, $\omega_{GAM}^2 = \left(\frac{7}{4} + \tau \right) \frac{v_t^2}{R_0^2}$, which is the same GAM dispersion relation obtain using MHD with a double adiabatic closure (Smolyakov *et al.* 2008). GAMs are special types of sound waves and as sound waves, their frequency strongly depends on the equilibrium pressure. Considering the MHD description of GAMs with a double adiabatic closure, χ in our work, is equivalent to the ratio $\frac{p_{\perp,0}}{p_{\parallel,0}}$, with $p_{\perp,0}$ the equilibrium perpendicular pressure and $p_{\parallel,0}$ the equilibrium parallel pressure. So increasing χ for a fixed $p_{\parallel,0}$, equals changing the equilibrium perpendicular pressure, which directly modifies the GAM frequency due to its dependence on the equilibrium pressure. This explains the global growing dependence of both the growth rate and frequency on χ , which is going to be evident on the figures below. The GAM frequency can be written in terms of the equilibrium parallel and perpendicular pressure as follows (neglecting τ), where ρ_0 is the equilibrium mass density.

$$\omega_{GAM}^2 = \left(\frac{3}{2} + \frac{p_{\perp,0}}{p_{\parallel,0}} + \frac{p_{\perp,0}^2}{p_{\parallel,0}^2} \right) \frac{p_{\parallel,0}}{\rho_0 R_0^2} \quad (3.14)$$

The dispersion relation equation (3.9) can be written in the form below by substituting equations (3.10), (3.11), (3.12) in (3.9).

$$\frac{1}{b\tau} \left[\frac{1}{q^2} + \frac{1}{2} + \chi + y^2 + \left(y^3 + y\chi + \frac{\chi^2}{2y} \right) Z(y) \right] + \left[\frac{1}{q^2} + \frac{1}{2} + \chi + \frac{yZ(y)}{q^2} + \left(\frac{y}{2} + y\chi + \frac{\chi^2}{2y} \right) + \frac{\chi^2}{4} Z(y)^2 \right] = 0 \quad (3.15)$$

Asymptotic behavior: Case $\tau \rightarrow 0$

In this limit, the first term in the square bracket is large compared to the second term. Neglecting this second term, we recover the dispersion relation in Ren & Cao (2014).

$$\frac{1}{q^2} + \frac{1}{2} + \chi + y^2 + \left(y^3 + y\chi + \frac{\chi^2}{2y} \right) Z(y) = 0 \quad (3.16)$$

Figure 1 shows the frequency and growth rate obtained from the complete dispersion relation (3.9) (blue curve) and the same quantities obtained in the $\tau \rightarrow 0$ limit (red curve).

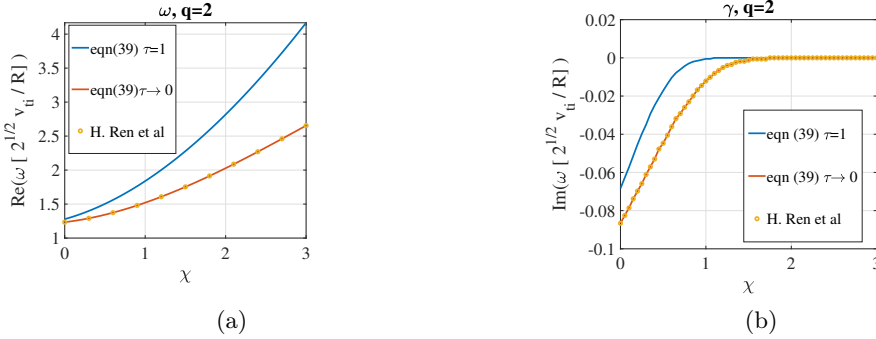


FIGURE 1. (a)Frequency (b)Growth rate

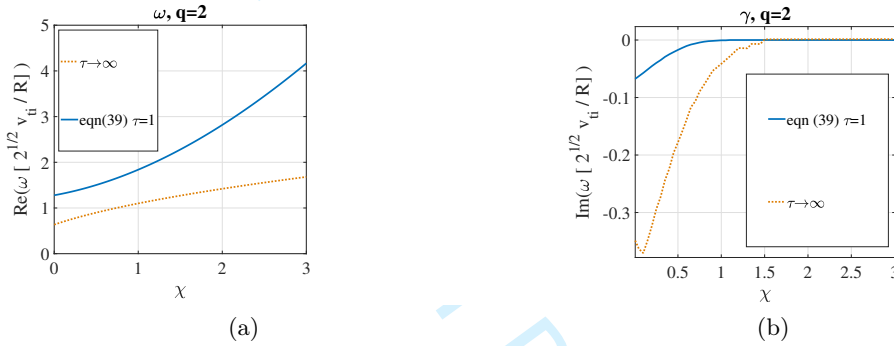


FIGURE 2. (a)Frequency (b)Growth rate

Asymptotic behavior: Case $\tau \rightarrow \infty$

In this limit, the terms in the second square bracket in equation (3.15) are larger in comparison to those in the first. So the dispersion relation reduces to,

$$\frac{1}{q^2} + \frac{1}{2} + \chi + \frac{yZ(y)}{q^2} + \left(\frac{y}{2} + y\chi + \frac{\chi^2}{2y} \right) + \frac{\chi^2}{4} Z(y)^2 = 0 \quad (3.17)$$

Figure 2 shows the frequency and growth rate obtained from the complete dispersion relation (3.9) (blue curve) and those obtained in the $\tau \rightarrow \infty$ limit (red dashed curve).

In the following sections, we solve the complete dispersion relation, equation (3.9), with values of τ , which are more realistic for tokamak plasmas.

3.3. Effect of ion temperature anisotropy on GAM frequency and growth rate

The GAM frequency and growth rate increase with χ (figure 3). However, the growth rate saturates for values of the parameters for which the instability becomes marginally stable. This saturation occurs at lower values of χ for higher values of q . It should be noted that the growth rate at higher values of q is overestimated, since damping effects due to finite orbit width are not considered in our model. These effects tend to be more important when q increases (Biancalani *et al.* 2014). Similar results were obtained in (Ren & Cao 2014). The regime of validity of our model is the plasma core. This is the region of excitation of energetic particle induced GAMs (EGAMs). Incidentally, the zonal flow residual level (Cho & Hahm 2021) can be enhanced by the anisotropic energetic particle

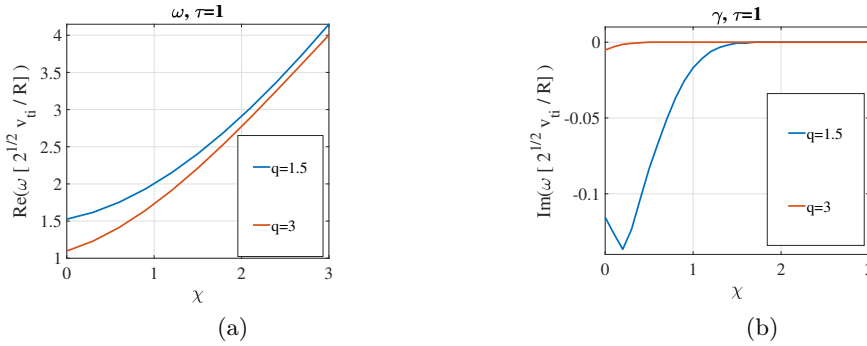
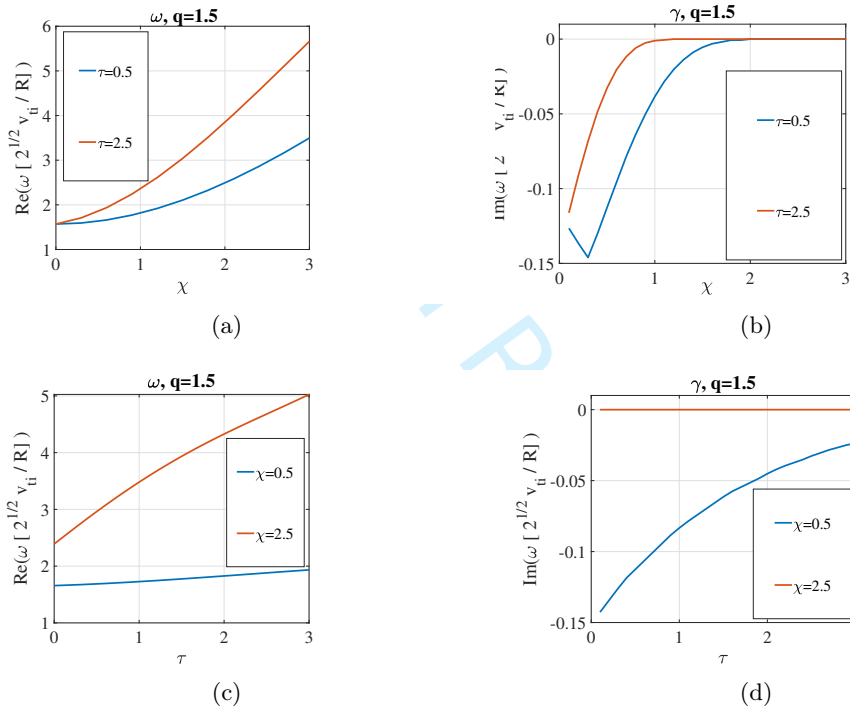


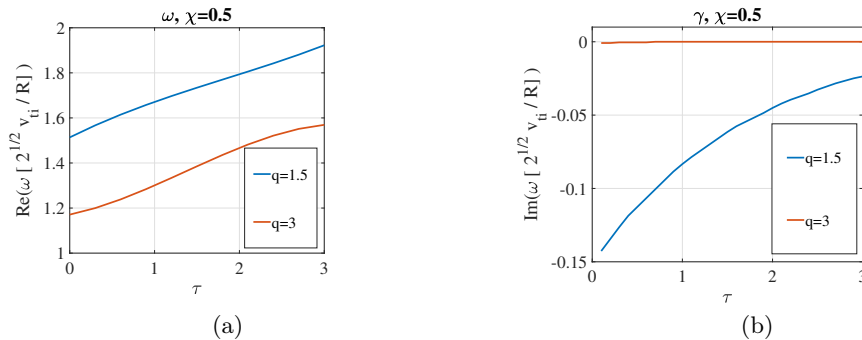
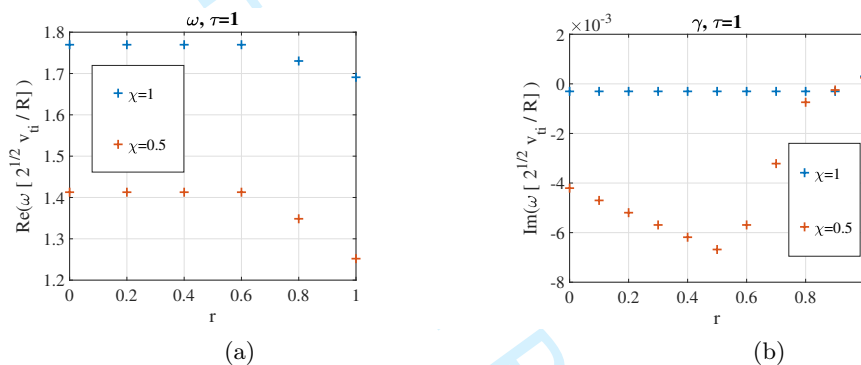
FIGURE 3. (a) Frequency (b) Growth rate

FIGURE 4. Effects of τ

distribution dominated by barely passing/barely trapped particles or by deeply trapped particles (Lu *et al.* 2019).

3.4. Effects of electron to ion temperature ratio

In this section, we study the effect of a finite τ (this parameter was neglected in Ren & Cao (2014)). Figures 4 (a) and (b), show the effects of χ on GAM frequency and growth rate for two different values of τ . We observe, as expected that, these quantities are increasing functions of χ . However, there is a significant increase in frequency and growth rate with τ . Figures 4 (c) and (d), show the variation of GAM frequency and growth rate with τ , for two values of χ . We recover the isotropic τ dependence of GAMs (*i.e.* increasing frequency with increasing τ). This effect is more pronounced for higher

FIGURE 5. Effects of τ FIGURE 6. (a) Frequency versus radial position (r), (b) Growth rate versus radial position (r), for the set of parameters of potential experimental relevance discussed in section 4.

values of χ in the anisotropic case. Figure 5, shows the effect of τ , on GAM frequency and growth rate for two different values of the safety factor q and for a fixed χ . We observe stronger damping for smaller values of q . This confirms the fact that even in the anisotropic case, GAMs are more stable in the core than at the edge of the tokamak plasma, where the safety factor, q , has large values. We can conclude from Figures 4 and 5 that, GAM frequency and growth rate significantly increase with τ and neglecting this parameter can lead to an underestimation of the frequency and to an overestimation of the damping rate.

4. Application to an experimentally relevant case

In this section, we apply the theory we have developed to a case of likely experimental relevance. For simplicity, we consider the case where the electron to ion temperature ratio is one ($\tau = 1$), which is compatible with experimental conditions. Sasaki *et al.* (1997) studied the ion temperature anisotropy in the reverse field pinch device EXTRAP-T2. In that work, $\chi \sim 0.5$ was measured. We here assume such values of χ are comparable to those that can be measured in tokamaks. To plot the GAM frequency spectrum for this parameter values, we use the safety factor profile from the experimental benchmark test case selected for Non-Linear Energetic-particle Dynamics EuroFusion project for Asdex Upgrade (NLED-AUG) (Vlad *et al.* 2021). Figure 6 shows that, the frequency spectrum of GAM is very sensitive to the safety factor in the presence of ion anisotropy. This is

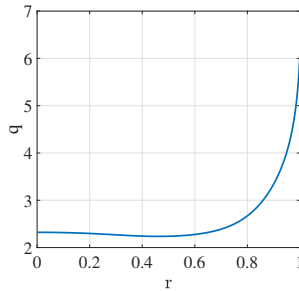


FIGURE 7. Safety factor profile

particular true closer to the plasma core where the GAM damping rate is almost an order of magnitude higher than in the isotropic case (damping due to finite orbit width which is important at higher values of q is not considered in this work). Even though GAMs are heavily damped in the core in the presence of anisotropy, as shown on figure 6, the core dynamic of GAMs is however important, since it can significantly modify the interaction of GAMs and energetic particle in the core, which leads to the so called EGAMs (Vannini *et al.* 2021; Rettino *et al.* 2022; Fu 2008).

5. Conclusion

Zonal structures are axisymmetric perturbations that are non-linearly generated by turbulence in fusion plasmas. There are two main types of zonal flows, namely, the zero frequency zonal flow (ZFZF) and its finite frequency counterpart, the geodesic acoustic mode (GAM). GAMs are unique to configurations with closed magnetic field lines with a geodesic curvature, like tokamaks. GAM frequency is of the order of the ion sound frequency, and its major damping mechanism in fusion plasma is collisionless damping (ion Landau damping). They are of interest to future magnetic fusion devices due to their potential role in regulating microscopic turbulence and its associated heat and particle transport.

In this work we revisited the linear gyro-kinetic theory of GAMs with adiabatic electrons described by a Maxwellian distribution function by including the effects of kinetic ions displaying a gyro-tropic temperature anisotropy modeled with a bi-Maxwellian distribution. We thus extended the linear GAM theory with an anisotropic ion temperature to include a general value of the electron to ion temperature ratio and we derived a general linear dispersion relation for an arbitrary ion distribution function. In the appropriate limit of a negligible electron to ion temperature ratio, we thus recovered the GAM dispersion relation in (Ren & Cao 2014). Solving the dispersion relation for the GAM frequency and damping rate for the more general case of interest here, we found that the ion temperature anisotropy yields non-negligible changes to both the GAM frequency and damping rate, as both tend to be increasing functions of $\chi = \frac{T_{\perp,i}}{T_{\parallel,i}}$. The ion Landau damping is confirmed to be stronger for smaller values of the safety factor. These features become more pronounced when a finite electron to ion temperature is considered. The values of the frequency and growth rate for a given χ , increase significantly as $\tau = \frac{T_e}{T_i}$, increases. Hence the effect of τ on GAM dynamics is not negligible and must be included in a complete model.

We applied our theory to a scenario of potential experimental relevance by using the safety factor profile from the NLED-AUG, experimental benchmark test case and assuming the ion temperature anisotropy in tokamaks is close to that measured in

the reversed field pinch device EXTRAP-T2. Plotting the frequency spectrum and the damping rate as function of position (while restricting for simplicity to the case of equal total electron and ion temperature), we find that in this scenario the core dynamics of GAMs is significantly modified in the presence of ion temperature anisotropy. Such a modification of the core dynamics of GAMs can impact the the interaction of GAMs and energetic particles in the plasma core.

In future works, we shall extend this linear theory of GAMs with inclusion of ion anisotropy effects in order to study the interaction of GAMs and energetic particle in the plasma core (EGAMs), since we have seen that the linear core dynamics of GAMs in relevant experimental scenario is significantly modified by the ion temperature anisotropy.

Acknowledgement

This work was partially supported by the "Lorraine Université d'Excellence" Doctorate fundings (project R01PKJUX-PHD21) belonging to the Initiative "I-SITE LUE" and by the R&D Program through Korea Institute of Fusion Energy (KFE) funded by the Ministry of Science, ICT and Future Planning of the Republic of Korea (No. KFE-EN2241-8). Part of this work has been carried out within the framework of the EUROfusion Consortium, funded by the European Union via the Euratom Research and Training Programme (Grant Agreement No.101052200 EUROfusion). Views and opinions expressed here are however those of the authors only and do not necessarily reflect those of the European Union or the European Commission. Neither the European Union nor the European Commission can be held responsible for them. Numerical calculations for this work have been partially performed on the cluster Explor of the "Maison de la simulation Lorraine" (We are grateful to the partial time allocation under the project No. 2019M4XXX0978), and on the MARCONI FUSION HPC system at CINECA. The authors are grateful to Etienne Gravier and Maxime Lesur (IJL, Nancy, France), to Guilhem Dif-Pradalier and Xavier Garbet (IRFM, CEA, France), to William Bin and Stefan Schmuck (ISTP, CNR, Italy), to Fulvio Zonca (CNPS, Frascati, Italy), and to Xin Wang and Zhixin Lu (IPP, Garching, Germany) for useful discussions and remarks.

REFERENCES

- BIANCALANI, A., BOTTINO, A., LAUBER, PH. & ZARZOSO, D. 2014 Numerical validation of the electromagnetic gyrokinetic code nemorb on global axisymmetric modes. *Nucl. Fusion* *54* 104004 .
- CERRI, S. S., HENRI, P., CALIFANO, F., DEL SARTO, D., FAGANELLO, M. & PEGORARO, F. 2013 Extended fluid models: Pressure tensor effects and equilibria. *Physics of Plasmas*, *20*, 112112 .
- CHAKRABARTI, N., GUZDAR, P. N., KLEVA, R. G., SINGH, R., P. K. KAW AND, V.NAULIN & RASMUSSEN, J. J. 2010 Geodesic acoustic mode in toroidal plasma. *AIP Conference Proceedings* *1308*, 108 .
- CHEN, L. & ZONCA, F. 2007 Nonlinear equilibria, stability and generation of zonal structures in toroidal plasmas. *Nucl. Fusion* *47* 886–891 .
- CHO, Y. W. & HAHM, T. S. 2021 Effect of temperature anisotropy on residual zonal flow level. *Phys. Plasmas* *28*, 052303 .
- CONWAY, G.D., SMOLYAKOV, A.I. & IDO, T. 2022 Geodesic acoustic modes in magnetic confinement devices. *Nucl. Fusion* *62* 013001 .
- DEL SARTO, D. & PEGORARO, F. 2018a Shear-induced pressure anisotropization and correlation with fluid vorticity in a low collisionality plasma. *Monthly Notices of the Royal Astronomical Society*, *475*, 181 .
- DEL SARTO, D. & PEGORARO, F. 2018b Shear-induced pressure anisotropization and

Effect of temperature anisotropy on the dynamics of geodesic acoustic modes 13

- correlation with fluid vorticity in a low collisionality plasma. *Un Comptes-Rendus de la 21e Rencontre du Non Linéaire, Paris 2018*, edited by E Falcon, M. Lefranc, F. Ptrluis, and C.-T. Pham (Université Paris Diderot, Non-Linéaire Publications, Paris, France, 2018) **21**, 13–18.
- DEL SARTO, D., PEGORARO, F. & CALIFANO, F. 2016 Pressure anisotropy and small spatial scales induced by velocity shear. *Physical Review E*, **93**, 053203 .
- FU, G. Y. 2008 Energetic-particle-induced geodesic acoustic mode. *PRL* **101**, 185002 .
- GAO, ZHE 2013 Collisional damping of the geodesic acoustic mode. *Phys. Plasmas* **20**, 032501 .
- GARBET, X., FALCHETTO, G., OTTAVIANI, M., SABOT, R., SIRINELLI, A. & SMOLYAKOV, A. 2006 Coherent modes in the acoustic frequency range in tokamaks. *AIP Conference Proceedings* **871**, 342 .
- GIRARDO, J., ZARZOSO, D., DUMONT, R., GARBET, X., SARAZIN, Y. & SHARAPOV, S. 2014 Relation between energetic and standard geodesic acoustic modes. *Physics of Plasmas* **21**, 092507 .
- GRANDGIRARD, V., GARBET, X., EHRLACHER, CH., BIANCALANI, A., BOTTINO, A., NOVIKAU, I., ASAH, Y., CASCHERA, E., DIF-PRADALIER, G., DONNEL, P., GHENDRIH, PH., GILLOT, C., LATU, G., PASSERON, CH., SARAZIN, Y. & ZARZOSO, D. 2019 Linear collisionless dynamics of the gam with kinetic electrons: Comparison simulations/theory. *Phys. Plasmas* **26**, 122304 .
- HASEGAWA, A., MACLENNAN, C. G. & KODAMA, Y. 1979 Nonlinear behavior and turbulence spectra of drift waves and rossby waves. *The Physics of Fluids* **22**, 2122 .
- HASSAM, A. B. & KLEVA, R. G. 2011 Double adiabatic theory of collisionless geodesic acoustic modes in tokamaks. *arXiv:1109.0057* .
- HOLE, M. J., VON NESSI, G., FITZGERALD, M, MCCLEMENTS, K. G., SVENSSON, J. & THE MAST TEAM 2001 Equilibrium analysis of tokamak discharges with anisotropic pressure. *Plasma Phys. Control. Fusion* **43** 1441–1456 .
- HOLE, M J, VON NESSI, G, FITZGERALD, M, MCCLEMENTS, K G, SVENSSON, J & THE MAST TEAM 2011 Identifying the impact of rotation, anisotropy, and energetic particle physics in tokamaks. *Plasma Phys. Control. Fusion* **53** 074021 .
- KAUFMAN, A. N. 1960 Plasma viscosity in a magnetic field. *Phys. Plasmas* **3**, 610 .
- LU, Z X., WANG, X., LAUBER, PH., FABLE, E., BOTTINO, A., HORNSBY, W., HAYWARD-SCHNEIDER, T., ZONCA, F. & ANGIONI, C. 2019 Theoretical studies and simulations of mode structure symmetry breaking in tokamak plasmas in the presence of energetic particles. *Plasma Phys. Control. Fusion* **61** 044005 .
- MACMAHON, A. 1965 Finite gyro radius corrections to the hydromagnetic equations for a vlasov plasma. *Phys. Plasmas* **3**, 610 .
- MING, Y., ZHOU, D. & WAMG, W. 2018 Geodesic acoustic modes in tokamak plasmas with anisotropic distribution and a radial equilibrium electric field. *Plasma Sci. Technol.* **20** 085101 .
- NOVIKAU, I., BIANCALANI, A., BOTTINO, A., CONWAY, G. D., GURCAN, O. D., MANZ, P., MOREL, P., POLI, E., A. DI SIENA, I & TEAM, ASDEX UPGRADE 2017 Linear gyrokinetic investigation of the geodesic acoustic modes in realistic tokamak configurations. *Physics of Plasmas* **24**, 122117 .
- QIU, Z., CHEN, LIU & ZONCA, F. 2009 Collisionless damping of short wavelength geodesic acoustic modes. *Plasma Phys. Control. Fusion* **51** 012001 .
- REN, H 2015 Geodesic acoustic mode in anisotropic plasma with heat flux. *Phys. Plasmas* **22** 102505 .
- REN, H. & CAO, J. 2014 Geodesic acoustic mode in anisotropic plasmas using adiabatic model and gyro-kinetics equation. *Physics of Plasmas* **21**, 122512 .
- RETTINO, B., HAYWARD-SCHNEIDER, T., BIANCALANI, A., BOTTINO, A., LAUBER, PH., CHAVDAROVSKI, I., VANNINI, F. & JENKO, F. 2022 Gyrokinetic modelling of anisotropic energetic particle driven instabilities in tokamak plasmas. *arXiv:2201.03836* .
- SASAKI, K, HORLING, P., FALL, T., BRZOZOWSKI, J. H., BRUNSELL, P., HOKIN, S., TENNFORS, E., SALLANDER, J, DRAKE, J. R., INOUE, N, MORIKAWA, J., OGAWA, Y. & YOSHIDA, Z. 1997 Anisotropy of ion temperature in a reversed-field-pinch plasma. *Plasma Phys. Control. Fusion* **39** 333–338 .

- SMOLYAKOV, A.I., GARBET, X., FALCHETTO, G. & OTTAVIANI, M. 2008 Multiple polarization of geodesic curvature induced modes. *Physics Letters A* 372 6750–6756 .
- SUGAMA, H. & WATANABE, T.H 2006 Collisionless damping of geodesic acoustic modes. *J. Plasma Phys.* 72 825 .
- THOMPSON, W. B. 1961 The dynamics of high temperature plasmas. *Phys. Plasmas* 3, 610 .
- VANNINI, F., BIANCALANI, A., BOTTINO, A., HAYWARD-SCHNEIDER, T., LAUBER, P., MISHCHENKO, A., POLI, E., VLAD, G. & TEAM, ASDEX UPGRADE 2021 Gyrokinetic investigation of the nonlinear interaction of alfvén instabilities and energetic particle-driven geodesic acoustic modes. *Physics of Plasmas* 28, 072504 .
- VLAD, G., WANG, X., VANNINI, F., BRIGUGLIO, S., CARLEVARO, N., FALESSI, M. V., FOGACCIA, G., FUSCO, V., ZONCA, F., BIANCALANI, A., BOTTINO, A., HAYWARD-SCHNEIDER, T. & LAUBER, PH. 2021 A linear benchmark between hymagyc, mega and orb5 codes using the nled-aug test case to study alfvénic modes driven by energetic particles. *Nucl. Fusion* 61 116026 .
- WINSOR, N., JOHNSON, J.L. & DAWSON, J. M. 1968 Geodesic acoustic waves in hydromagnetic systems. *Physics of Fluids* 11, 2448 .
- ZARZOSO, D., GARBET, X., SARAZIN, Y., DUMONT, R. & GRANDGIRARD, V. 2012 Fully kinetic description of the linear excitation and nonlinear saturation of fast-ion-driven geodesic acoustic mode instability. *Phys. Plasmas* 19, 022102 .
- ZHANG, M & ZHOU, D 2010 Magnetic components of geodesic acoustic modes in plasmas with anisotropic ion distribution. *Plasma Sci. Technol.* 12 6-10 .
- ZONCA, F. & CHEN, L. 2008 Radial structures and nonlinear excitation of geodesic acoustic modes. *EPL* 83 35001 .
- ZONCA, F., CHEN, L. & SANTORO, R.A 1996 Kinetic theory of low-frequency alfvén modes in tokamaks. *Plasma Phys. Control. Fusion* 38 2011 .